Timing

Andrea Grossutti, mat. 1237344 Alessandro Lovo, mat. 1236048 Leonardo Zampieri, mat. 1237351

November 26, 2019

1 Aims

- Energy calibration of the organic scintillators and calculation of the energy resolution from the analysis of the Compton edge;
- Optimization of the external delay of the analogue CFTD to obtain the best time resolution;
- Study of the time resolution behaviour as a function of the energy;
- Comparison between the timing resolutions obtained from analogue and digital treatment of the signals;
- Measurement of the speed of light.

2 Experimental setup

The experimental setup consist of two collinear organic scintillators, mounted on a sledge, and a ²²Na source collimated between two lead bricks.

Data are collected from the detectors through a electronic chain: a fan-in-fan-out quad module replies the signal of each detector and produces four copies of it; then, through a CFD, a trigger signal is produced. The CFD trigger threshold has been set so that the background noise is discarded, while the interesting signals produce an output.

3 Apparatus calibration

Both the detectors and the TAC need to be calibrated. Firstly, let's calibrate the detectors.

A spectra for each detector is acquired; due to the composition of the detector, the photopeaks are negligible and only the compton effect are detected. Through the position of the compton edge (CE), the calibration can be done.

Detector 1 25000 15000 10000 2000 4000 6000 8000 10000 12000 14000 16000 18000

Figure 1: Det 1: Position of CE's centroids and widths

Channel

The gaussian fit way was discarded, due to its strongly dependence from fit range choice. After a proper spectra rebinning, then for each CE the position of the maximum c_{ch} and the half width half maximum w_{ch} in channels have been found (fig 1, tab 1)*. The observed CE is a convolution of a real CE with a gaussian noise whose width is proportional to the resolution of the detector σ_{res} ; this convolution results in a shift of the maximum of the CE towards lower energies. By simulating effects on CE varying σ_{res} we compute the simulated resolution $r_{sim} = \frac{w_{sim}}{c_{sim}}$ and correlate it with c_{sim} , i.e the peak position in energy (fig 2).

If we assume the calibration relation E = a * ch + b, then the resolution in energy is:

$$r_E = \frac{w_E}{c_E} = \frac{aw_{ch}}{ac_{ch} + b} = \frac{w_{ch}}{c_{ch} + b/a}$$

So we first assume b/a = 0 to compute r_E , and then by imposing $r_E = r_{sim}$ we can find the peak positions in energy c_E allowing us to compute a and b via linear fit. We can now update the value of r_E and repeat the process. After a few iterations the process converges and gives us the results in tab 2.

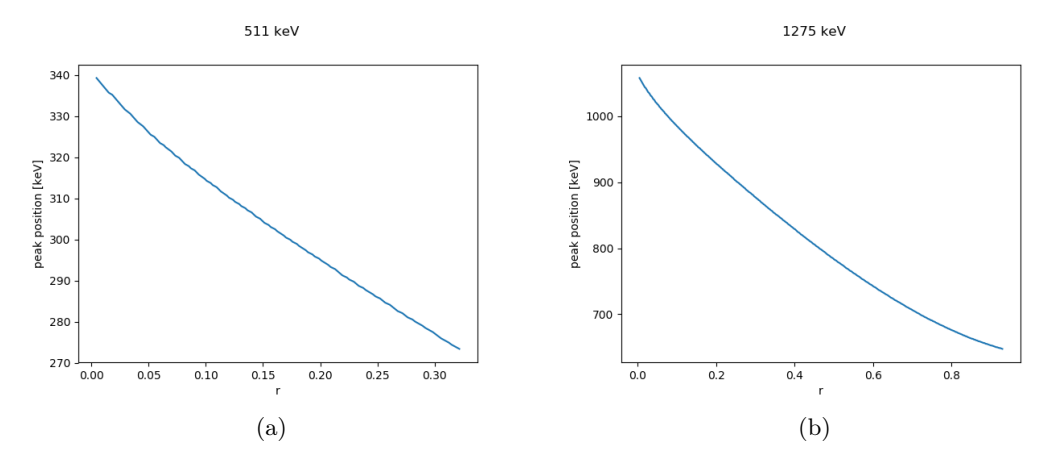


Figure 2: Relation between the resolution of the peak and the peak position

^{*}As described in Dietze, Klein: Gamma-calibration of NE 213 scintillation counters, Nuc. Instr. and Meth., 193 (1982), https://doi.org/10.1016/0029-554X(82)90249-X

Det	photopeak [keV]	c_{ch}	w_{ch}	$c_E [\text{keV}]$
#1	511	3440 ± 9	832 ± 13	283.6 ± 0.8
	1275	11312 ± 9	960 ± 13	992.9 ± 0.7
#2	511	4400 ± 9	896 ± 13	286.2 ± 0.7
	1275	13392 ± 9	960 ± 13	1000.5 ± 0.7

Table 1: Centroids and widths of the CE peaks: the errors for the values in channels come from a uniform distribution on the bin width of the histogram. The value of c_E here is the one after the calibration process converged

Det	a [keV]	b [keV]
#1	0.0901 ± 0.0002	-26 ± 2
#2	0.0794 ± 0.0002	-63 ± 2

Table 2: Calibrations coefficients after the calibration process converged

Even the TAC must be calibrated. The system is setup with a delay module just before the TAC stop. Multiple events are acquired with different delays, and centroid of each peak are found.

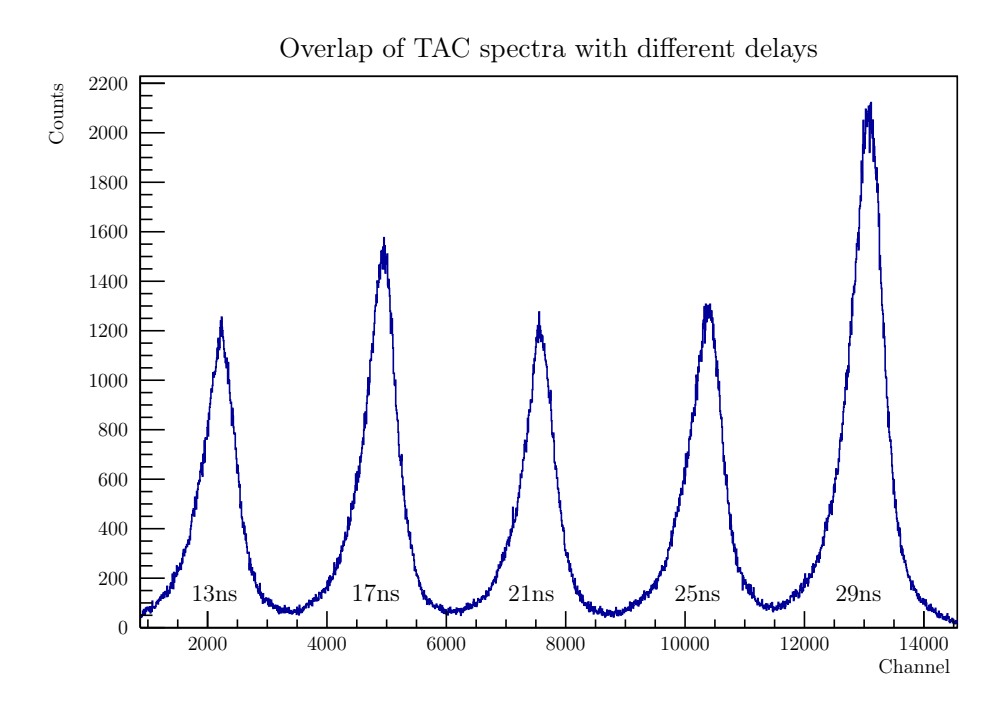


Figure 3: Different peaks with different delays.

Delay [ns]	Centroid [channel]
13	2235 ± 20
17	4950 ± 30
21	7555 ± 30
25	10390 ± 30
29	13080 ± 40

Table 3: TAC centroids. Different height of the peaks are due to different acquiring time.

The found centroid are fitted using a linear relation (the χ^2 value confirm the linear dependence):

$$t = m \cdot \text{channel} + q$$

 $m = (1.477 \pm 0.005) \text{ps}$

where the q value isn't reported, having no meaning. In fact, delays are introduced in a more complex system, which already have an internal delay: zero external delay therefore doesn't mean zero time in TAC.

4 LEMO calibration

A set of LEMO cables is provided. Setting external delay to 13ns and inserting one by one each LEMO cable in series with the external delay module, 5-minutes datasets are acquired; computing the difference between the observed centroids and the centroid without LEMO cable previously measured, and converting it with the calibration parameter, the time-length of each LEMO cable is computed.

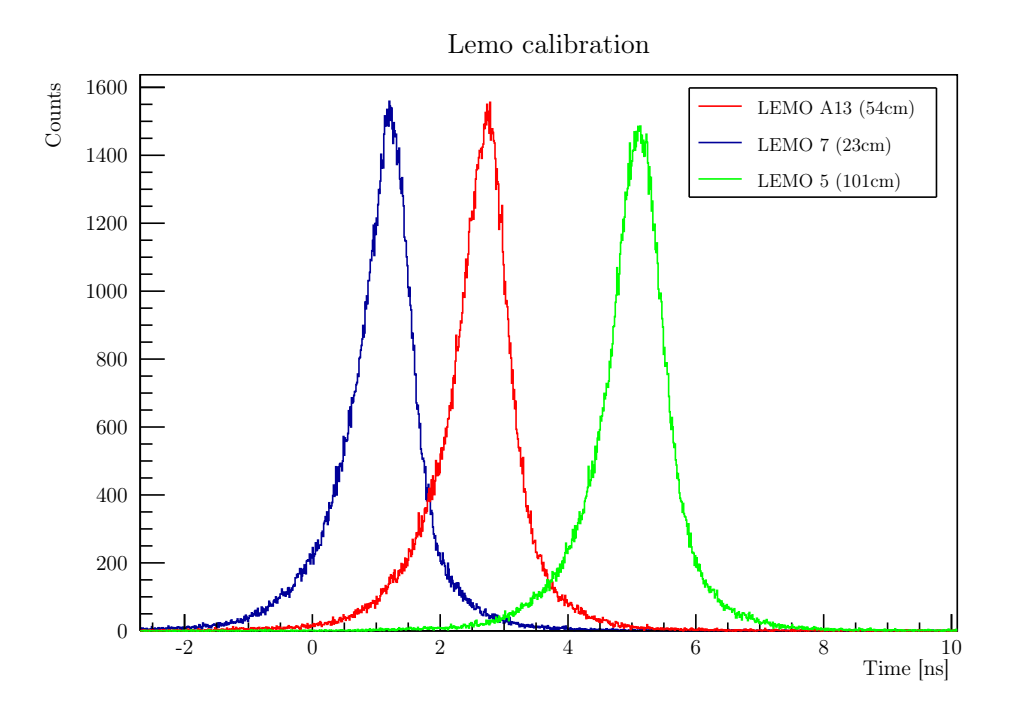


Figure 4: Some of the peaks of the LEMO cables

LEMO ID	LEMO length [cm], ± 0.1	LEMO time
7	23.0	1.15 ± 0.04
6	22.5	1.17 ± 0.04
13	53.5	2.71 ± 0.05
5	101.0	5.08 ± 0.07
4	101.0	5.12 ± 0.04
2	53.5	2.70 ± 0.03

Table 4: LEMO cables

LEMO correlation length - time

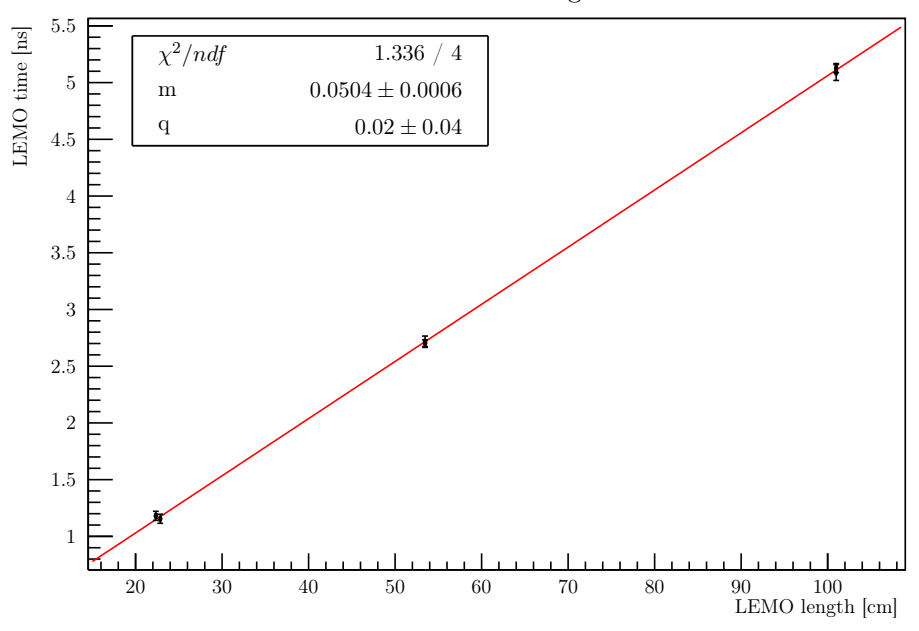


Figure 5: Relation between LEMO length and time: as expected, the dependence is confirmed.

5 CFD delay optimization

The CFD is provided by an external delay to properly superimpose a delayed copy of the signal to a inverted reduced one. This delay must be properly set to optimize the TAC resolution. With only the preset delay, the signal detected by the TAC is large and not gaussian (see fig. 6); after some tests, a setup which lead to a better resolution and a more gaussian-like output is obtained.

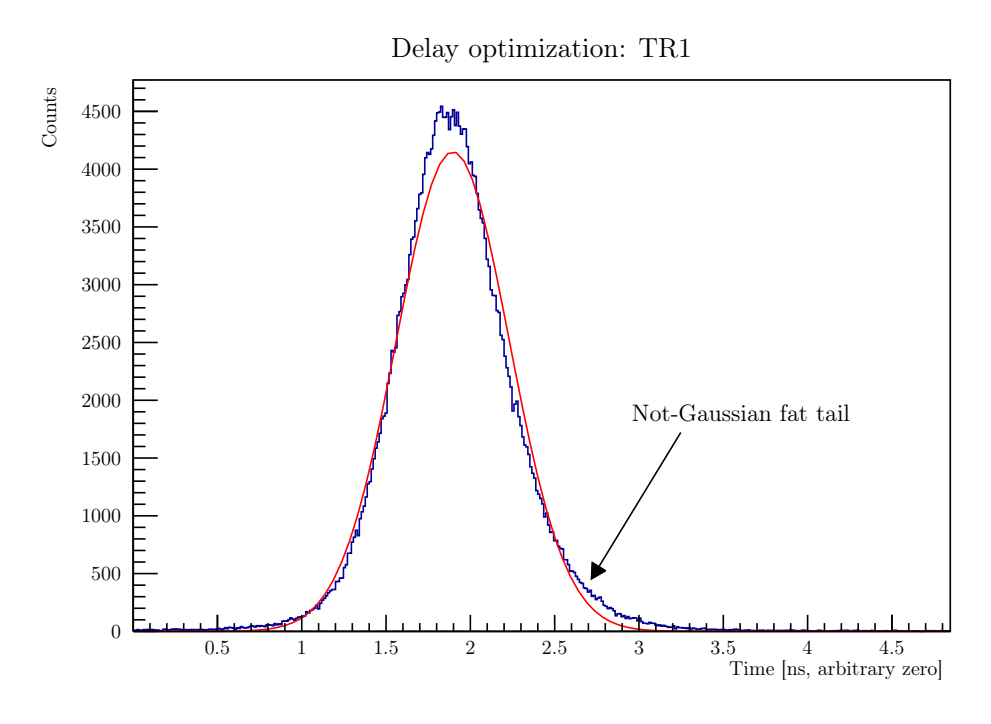


Figure 6: Initial situation: large not-guassian shape.

Different combination of LEMO cable has been inserted in series with the pre-set delay; every time the configuration changed, the WALK ADJ potentiometer has been regulated to minimize the

dispersion (see fig. 7).

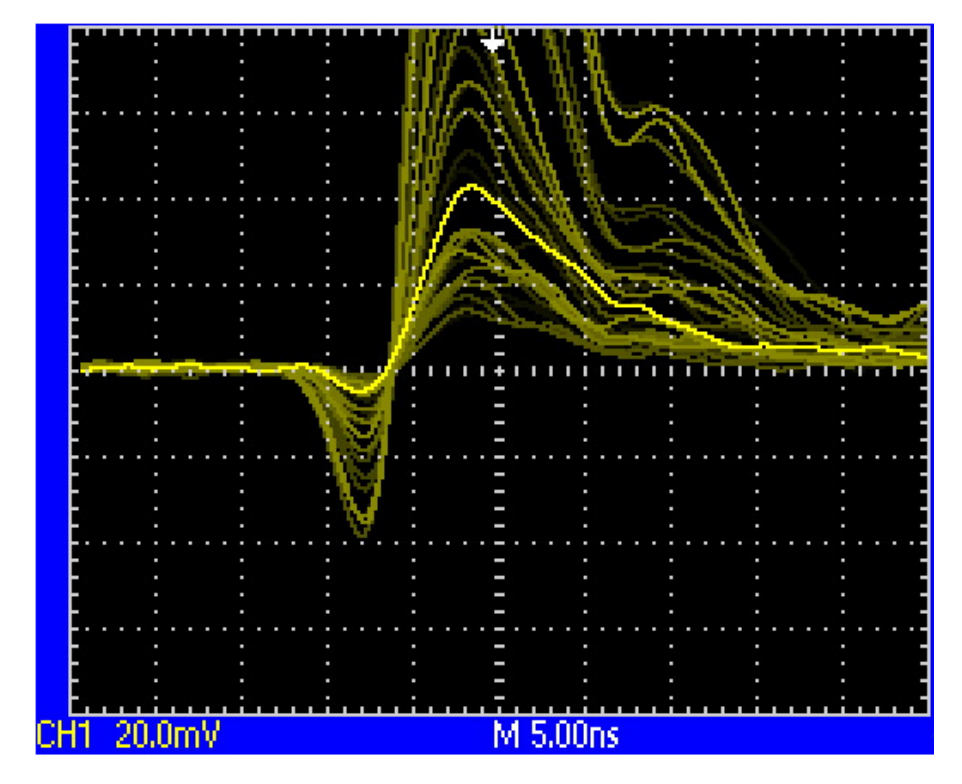


Figure 7: Monitor CFD signal triggered on CFD output, seen by the oscilloscope.

Fitting the obtained peaks with gaussian and relating them to the delay inserted in the CFDs (after some tests, we noticed that the optimal setup is with the same delay in both the CFD), the figure 8 is obtained. As can be seen from the figure, a minimum is found at about 3ns of delay (LEMO 13 and 2 for detector 1 and 2, respectively). Considering the pre-set delay (around 2ns), this lead to a optimal delay of around 5ns, that is about 80% the rise time (~ 6 ns) as expected.

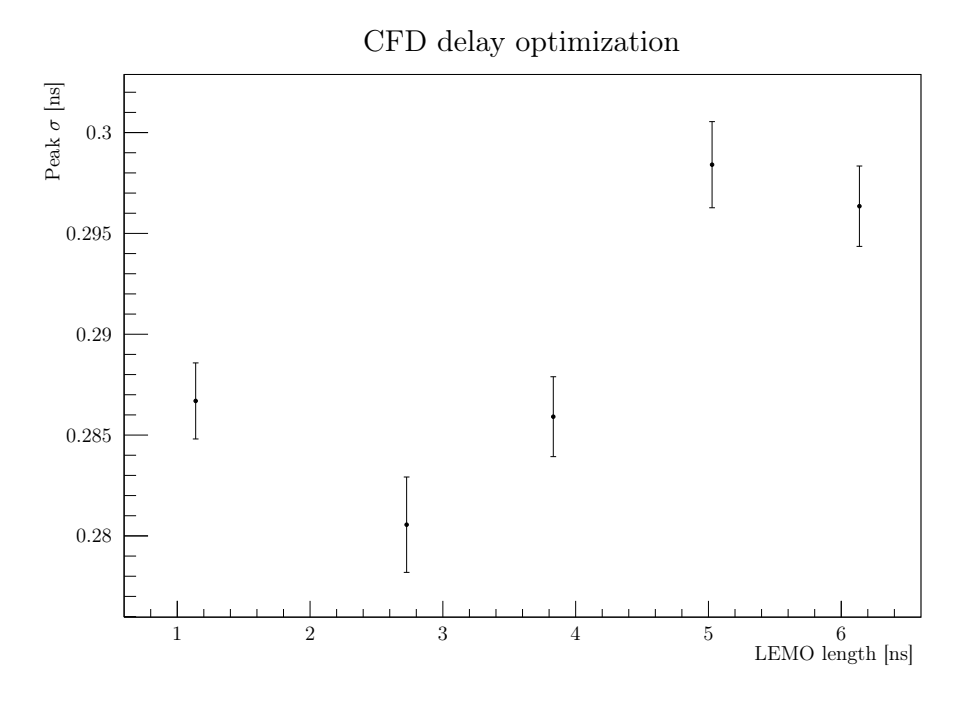


Figure 8: Optimization of the CFD delay.

The minimum configuration has been kept for all the following Measurements.

6 Time resolution in function of energy range

In order to have a larger compton energy spectra, we acquired 20 hours of data using a 60 Co. This source decays emitting two photons of energy around 1MeV: a few of them are emitted back-to-back and hence can trigger the coincidence unit (fig 9).

We can now proceed by filtering in energy the spectra and looking how the resolution of the TAC peak behaves. Since the TAC peak has a fat-tailed distribution, the gaussian fit is far from accurate, so we used the Full Width Half Maximum (FWHM) as a quantifier of the resolution of the peaks. The filtering can be done either by setting a Lower Energy Threshold (LET) or by selecting a window in energy, i.e. keeping only the data between the LET and an Upper Energy Threshold (UET). The results are shown in fig 10.

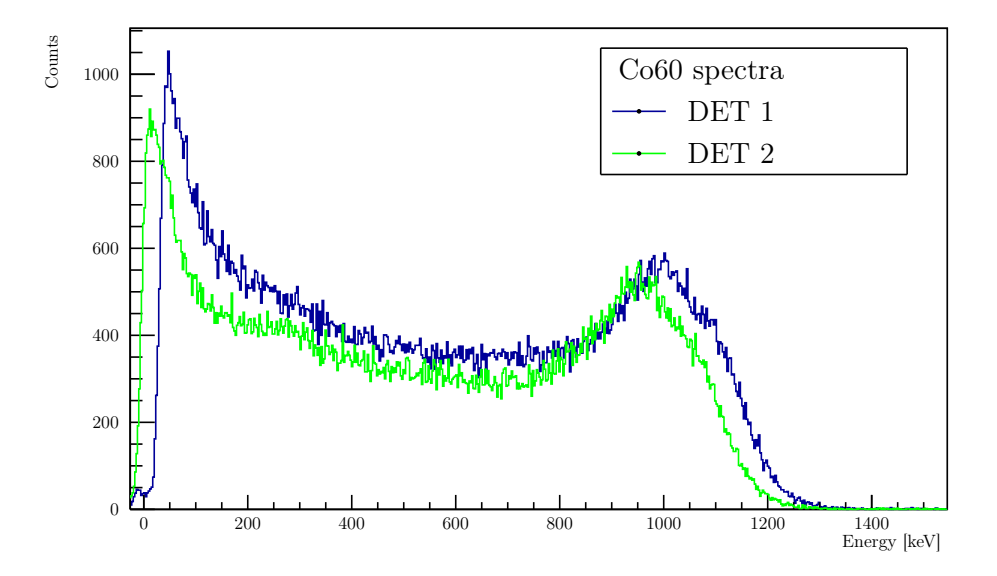


Figure 9: Energy spectra of the two detectors with ⁶⁰Co source.

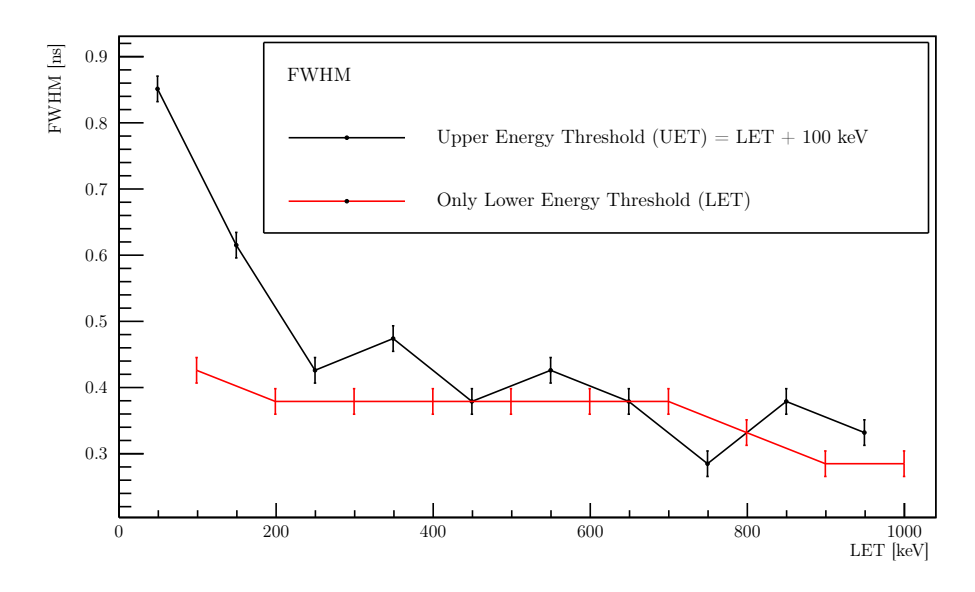


Figure 10: When computing the FWHM the peaks had been properly rebinned in order to have them sufficiently smooth. The errors on the FWHMs come from a uniform distribution on the bin width.

7 Speed of light

The detectors have been placed such that they're about 170m away. The source has been placed firstly near the detector 1 and then near the detector 2, and the TAC signal has been acquired; therefore, the centroids μ_1 and μ_2 of the two measurements have been found through a gaussian interpolation. Measuring the distance between the two source positions d, the light speed can be computed. Observe that the two centroids have been firstly subtracted and then calibrated, to preserve the resolution.

The errors has been propagated as casual errors. Note the high error on the distance between the positions of the source, due to the width of the source.

$$\mu_1 = (16433 \pm 2)$$

$$\mu_2 = (8966 \pm 2)$$

$$d = (161.9 \pm 0.5) \text{cm}$$

$$c = \frac{2d}{(\mu_1 - \mu_2)m} = (2.94 \pm 0.01) \cdot 10^8 \text{m s}^{-1}$$